Chapter 6

Anchoring Transition and Influence of Director Fluctuations in Liquid Crystal Droplets

6.1 Introduction

Polymer-dispersed liquid crystals (PDLC) [1] are a relatively new class of materials that hold promise for many applications ranging from switchable windows to projection displays. These materials, which are simply provide useful boundary condition for nice spherical LC droplets, are the focus of extensive research in the display industry. PDLCs consist of liquid crystal droplets that are dispersed in a solid polymer matrix. The resulting material is a sort of "swiss cheese" (Figure 6.1) polymer with liquid crystal droplets filling in the holes. These tiny droplets (a few microns across for practical applications) are responsible for the unique behavior of the material. By changing the orientation of the liquid crystal molecules with an electric field, it is possible to vary the intensity of transmitted light. These system are of great interest in technology for display [2]. These systems have been subjected of considerable research, especially from the point of view of understanding the physics of the different structures that can be formed.

Deuterium NMR was used to study submicron-size droplets of monomeric liquid crystal dispersed in solid polymer matrix [3], with special focus on the director fluctuations were monitored too. The deformations were also investigated in a PDLC sample, by applying a varying electric field was applied in addition to the magnetic filed of the NMR [4]. It was shown that for droplets of size larger than 0.35 μm (diameter) N-I transition is first

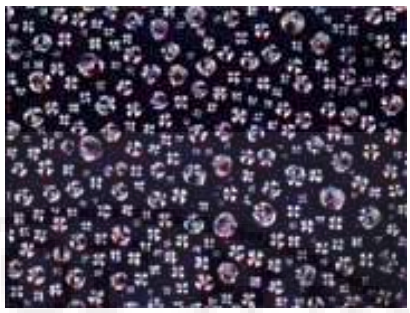

Figure 6.1: An illustrative picture of PDLC

order; and for lesser than 0.35 μm it is continuous with a paranematic phase. The deformations of spherical droplet shapes into randomly oriented rotational ellipsoids were also investigated both by theoretical and experiential methods. The orientational order in stretched polymer dispersed liquid crystal was investigated using deuterium NMR in the nematic and in isotropic phases [5]. It shows that the surface value of the order parameter turns out to be largely temperature independent and is seen to increase with increasing strain. Light scattering and electro – optic response was used to study micro – droplets of nematic liquid crystal which are spontaneously formed in a solid polymer at the time of polymerization [6]. Electro-optic properties of PDLC show a reversible optical response from an opaque state to a highly transmitting state under the action of an appropriate electric field which aligns the liquid crystal director [7]. Light control films consisting of submicron liquid crystal droplets dispersed in ultraviolet-cured polymer matrices, which can respond optically to both applied electric fields and temperature changes, were formed potentially useful for displays and light shutters [8]. The optomechanical properties of a polymer dispersed liquid crystal film were investigated by simultaneously measuring the stress-strain and polarization dependent optical transmission characteristics. The polymer alignment at the interface increases the droplet order parameter along the stretch axis, consistent with the results of the optical and mechanical experiments [9].

Holographic polymer dispersed liquid crystal materials were studied using NMR and dynamic light scattering methods, which were prepared for switchable diffractive optical

elements [10]. Their reflection peaks were tuned as a function of applied voltage [11]. Theoretical studies showed stripe pattern formation when a holographic PDLC induced phase separation via anisotropic pattern photo-polymerization [12]. In real systems, the radial structure occurs more frequently than the diametrical ones. Continuous structure transitions in a spherical chiral nematic droplet under the influence of an electric field was studied [13]. Cholesteric liquid crystal droplets embedded in a medium which enforce parallel surface anchoring was treated. The Frank's free energy was minimized to study disclination lines of integer and half-integer values [14]. Theoretical studies on the stability of uniaxial nematic liquid crystalline structure in supra-micronm-size spherical cavities that impose a weal homeotropic anchoring were carried out [15]. These predicted a triple point of radial, non singular axial and axial structure. Such a droplet was also studied using scattering matrix and nematic differential cross section [16]. Scattering patterns were calculated in detail for the three different nematic director's configurations: one characteristic of a droplet in a strong external field, the other characteristic of a droplet outside the field in the case normal surface anchoring and their characteristics of an isotropic droplet with a surface induced nematic layer. Ordering in bipolar liquid crystal droplets was also studied close to the nematic – isotropic transition. The droplet structure was obtained by minimization of Landau-de-Gennes free energy [17]. It is observed that there was a growth of a polar defect toward the center of the droplet. Similarly a spherical submicrometer droplet embedded in a solid polymer was studied using Landau-de-Gennes theory [18]. For a droplet with a radial structure, the strength of the nematic polymer interfacial interaction affects the nematic – paranematic phase transition, and may in addition induce a boundary layer nematic phase. Rayleigh-Gans approximation was used to derive the scattering matrix, differential cross section and the total cross section for a small nematic droplet [19]. Earlier simulations [20] based on LL model have clearly shown that the size of this inner uniaxial core is independent of the actual size of the droplet (assuming that it is always bigger than the core region) [21], and it is essentially determined by the nature of the Hamiltonian chosen. To make this scenario quantitative, the concept of radial order parameter S_R was

introduced to specify the degree of alignment of the LC region along the radial direction of the droplet, along with S which denotes the uniaxial ordering of the nematic phase [20]. These simulations focused on the temperature dependence of the formation of the radial order, and its propagation to the inner layers, as the nematic phase is formed. Further studies were carried out on these droplets to understand the effects of applied external field [22] at various anchoring strengths at the polymer interface. Different molecular organizations were investigated by illustrating their influence on the simulated NMR spectra. Droplets with toroidal and bipolar boundary conditions were also studied using Monte Carlo simulation for different anchoring strengths and at different external fields [23] [24] [25] [26]. More recently a droplet of biaxial molecules was investigated using MC simulations based on a suitable lattice Hamiltonian [27] for the different kinds of defects formed in such systems [28].

A simple method for the simulation of the textures of nematic liquid droplets as observed through a polarization microscope was developed [29], using basic principles of transformation matrices in optics. When the system size is bigger than a particular size, experiments cannot readily be done, and in such cases simulations become very useful and important for studying such systems. Simulation studies were used to study the different structures and the defect formation in PDLC. To study the effect of different types of orders induced, different polymers that were modeled to give radial, toroidal, and bipolar order [20], [26]. A model droplet of 304 particles with radial order percolating in to the system due to the polymer was studied using Monte Carlo simulations [23]. The whole droplet was split in to shells of unit radius and numbered from the center of the droplet. Average energy and it derivative with temperature were studied to understand the transitions occurring in this system. Other than the above mentioned two parameters the system order parameter $< P_2 >$, the fourth order polynomial $< P_4 >$ and the radial order $< P_2 >_R$ were computed. These order parameters were computed for every shell of the droplet. The LL model [30] was used to simulate the system using the Metropolis algorithm, and the effect of anchoring strength 'J' was investigated [31]. It was seen that with changes in J the

radial order in the system changes dramatically. For higher values of J a hedgehog defect formation was observed in the center of the droplet which disappeared to give an ordered domain at lower anchoring strengths. A droplet in a polymer inducing toroidal surface order [25] was studied as a function of temperature, and with changes in the anchoring strength. Another study focussed on the effect of an external field on a droplet with radial order percolating due to the substrate interactions [32]. To understand this system better, NMR spectra (of ^{2}H nuclei attached to rigid core) were computed for different director organizations using Monte Carlo methods. At stronger fields the line-shape essentially reduces to a doublet corresponding to the parallel splitting, whereas at much lower fields it is the characteristic of a powder spectrum. A detailed simulation of NMR spectrum along with the order parameters were carried out to investigate the different molecular organizations comparable with external conditions. A similar study was done with the polymer matrix inducing a bipolar order, and here the external field magnitude was varied for both positive and negative susceptivity anisotropy [24]. Droplets were also modeled using Gay-Berne potential to induce radial order, and it was observed that radial order percolated only for large enough droplets [33]. Droplets with radial, bipolar, and random boundary conditions were also considered, and examined from the point of the influence of specific molecular motion on the ^{2}H NMR spectrum [34]. The effects of molecular motion such as fluctuations of molecular long axes and translational diffusion, and on external field ordering effects were computed [35]. Using NMR as a tool the development of a defect was observed in a droplet with bipolar boundary conditions [36]. When closer to the confining substrate diffusion is significantly slower than in the bulk liquid crystal, leading to in perceptible changes in the NMR spectra. Dynamic effects were calculated especially due to translational diffusion and on its slowing-down near the surface layer [37]. Molecular dynamics of a droplet placed at the liquid crystal interface between two different regions of the solid polymer matrix was studied.The interface accordingly separates the droplet into two hemispheres: the first of these is under radial boundary conditions; the second hemisphere is under bipolar boundary conditions were studied [38]. Using a simple model for

biaxial nematics [27], [39] a droplet was modeled [28]. Polarizing textures were used to study this system in comparison to uniaxial molecules for different boundary conditions.

In particular, these droplets of micrometer size, or less, were earlier investigated [18] under different anchoring conditions imposed by the bounding polymer matrix. The motivation originated both from the point of basic issues involved in determining the equilibrium structures in such soft model systems under confinement, as well as due to their applications as optical modulators [16] [29]. Of specific interest is a droplet subjected to radially ordering conditions at the polymer-substrate interface [23]. Markov chain Monte Carlo (MC) studies based on Lebwohl-Lasher (LL) model [30] show that the droplet, in its nematic phase and under strong anchoring conditions, is essentially radially ordered but for a small spherical region at the core which has the uniaxial nematic phase [22]. The origin of this core region is attributed to the delicate balance between energy penalty imposed by the radial ordering (at that curvature) and the energy expenditure involved in maintaining an interfacial spherical region (between the inner uniaxial ordering and outer radial ordering [31]). Obviously, this is dictated on one hand by the degree of the relevant elastic distortion sustainable (in this case the splay distortions) *vis-á-vis* the influence of the inter-molecular interactions to bring about uniaxial ordering.

One of the interesting questions that arises in this connection concerns the role of anchoring strength of the bounding surface in inducing radial order (at a given temperature in the nematic phase), and nature of the transition from a wholly uniaxial structure (when the bounding surface is completely ineffective in influencing the liquid crystal inside) to an essentially radial structure, as was observed in the earlier work under strong anchoring condition. The other important considerations include the role of the relevant elastic property (splay energy represented by the corresponding coefficient K_1) in determining the nature of this transition, the size of the inner uniaxial core that emerges, and also the extent of competition that it may provide at the interfacial region, betrayed by the fluctuations in the order parameters quantifying the equilibrium structure of the medium. In other words, use of a suitable Hamiltonian which can incorporate the elastic properties of the medium

while accounting for the nematic order of the liquid crystal would be very appropriate in the study of this problem. One of the questions addressed is whether the influence of the anchoring by the surface, and consequent induced radial order, could be viewed as due to a wetting phenomenon.

In this context, it may be noted that a lattice based Hamiltonian which explicitly takes into account, the elastic properties of the medium via the three elastic coefficients (splay (K_1), twist (K_2), and bend (K_3) elastic constants) was proposed earlier [40]. This interaction is computed for nearest neighbor lattice elements. Its application to Schadt-Helfrich cell was demonstrated through detailed Monte Carlo simulations [40]. In this work, we shall adopt this model to study the equilibrium director configurations of a PDLC droplet in its nematic phase under radial boundary conditions, with specific focus on anchoring transition induced by variable coupling to the polymer matrix, and the role of splay distortion.

6.2 Hamiltonian Used and Details of simulations

The model Hamiltonian used for this study is

$$\Phi_{jk} = \lambda \left[P_2\left(a_j\right) + P_2\left(a_k\right)\right] + \mu\left(a_j a_k b_{jk} - \frac{1}{9}\right) + \nu P_2\left(b_{jk}\right) + \rho\left[P_2\left(a_j\right) + P_2\left(a_k\right)\right] P_2\left(b_{jk}\right). \tag{6.2.1}$$

Here, P_2 is the second rank Legendre polynomial. The coefficients of expansion are related to the elastic constants through the following relations, involving the chosen linear dimension Λ of the volume element in the cubic lattice to represent their local directors:

$$\begin{aligned}
\lambda =& \frac{1}{3}\Lambda\left(2K_1 - 3K_2 + K_3\right) \\
\mu =& 3\Lambda\left(K_2 - K_1\right) \\
\nu =& \frac{1}{3}\Lambda\left(K_1 - 3K_2 + K_3\right) \\
\rho =& \frac{1}{3}\Lambda\left(K_1 - K_3\right).
\end{aligned} \tag{6.2.2}$$

An interesting feature of this potential is that Λ, enters as a length scale over which the director gradient is discretized and defines the lattice parameter corresponding to the distance between the neighboring sites. By setting all the elastic constants equal to each other, say K, the above potential is reduced to the form of the Lebwohl-Lasher potential. Under these special conditions, the energy scale parameter ϵ, is equal to ΛK for the present model. In general, the total free energy of the system is then given by

$$\Psi = \frac{1}{2}\sum_{j=1}^{N}\sum_{k=1}^{6}\Phi_{jk}, \tag{6.2.3}$$

where N is the number of sites. Following the procedure adopted earlier, the scaled potential for use in simulations is obtained by dividing equation 6.2.1 by $|\nu|$. This leads to a scaled temperature, to be used in the Monte Carlo scheme, given by

$$T^* = k_B T/|\nu| = 3k_B T/(\Lambda|K_1 - 3K_2 - K_3|). \tag{6.2.4}$$

A detailed description of this Hamiltonian is discussed in the Chapter 1 of this thesis.

A sufficiently large cubic lattice is considered and a sphere of chosen radius (in lattice units) is carved out [22]. Consequently the bounding surface will be a jagged sphere due to the discrete nature of the arrangement of lattice points. Each lattice point is associated with a local director say, spin averaged over molecules enclosed in the cubic volume element of dimension Λ. Each spin is associated with a unit vector oriented along that local director. The lattice sites inside the sphere represent local directors within the liquid crystal which participate in the Monte Carlo chain dynamics, while those outside the sphere with fixed desired orientations correspond to substrate imposing the required boundary conditions (in the present case, oriented towards the center so as to impose radial boundary conditions surface anchoring). These fixed molecules, representing the substrate, hence do not participate in the simulation moves.

The flexibility of this Hamiltonian is utilized to study the effect of elastic properties on the director distribution by taking the example of a liquid crystal with known elastic constants in the nematic medium for purposes of simulation in this work. Thus, we set the

values of K_1, K_2, and K_3 from the measurements on PAA taken at a reduced temperature T/T_{NI} equal to 0.963 as $7.0 \times 10^{-12}N$, 4.3×10^{-12}N, and 17.0×10^{-12}N, respectively [40]. The energy scale is set, for a given set of elastic constants, by the dimension of the volume element over which the local director is defined, and hence the effective temperature at which the canonical ensemble is constructed is determined by this choice of equation 6.2.4. From the previous studies on planar hybrid film [44] it was concluded that the continuum results could be recovered for a choice of this dimension typically in the range of a few hundred $\mathring{A}$ and above, corresponding to a typical reduced temperature T^* of 0.10 and below. Assignment of lower values of Λ, leading to higher values of T^*, would correspond to, in physical terms, appreciable fluctuations in the director field. It was found that for such effective high temperatures, the predicted results were not consistent with the expected behavior from continuum theory based on minimization procedures. Typical value for Λ above which the fluctuations are small enough to yield satisfactory simulated results consistent with experimental results was reported to be around 700 $\mathring{A}$.

Due to the symmetry of the problem (nematic droplet subjected to radial boundary conditions) only splay distortion is operative, and this convenient situation is exploited by extending these studies as a function of relative splay energy contribution, effective by varying the value of K_1 relative to the other elastic constants. To this end, the simulations are performed for different K_1 values at fixed K_2 and K_3, and the results are then discussed for convenience in terms of the ratio (called scale factor, say α) of the assigned K_1 value to its actual value.

These studies are also aimed at examining the influence of the surface anchoring on changes in the director structure, and accordingly we introduce a variable anchoring strength ε_S (in units of the energy scale set above), ranging from 0 to 1. This defines the strength of interaction between the liquid crystal molecules and the (orientationally) fixed molecules in the substrate. Introduction of this variable facilitates a study of possible anchoring induced structural transitions in the system.

Different physical properties are computed based on these simulations, and in order

to get an insight into the director structure inside the droplet, we consider the droplet to be comprising of concentric shells of a given width indexing them in ascending order as we move away from the center of the droplet. We report ensemble averages of different properties measured within each of the layers. The variables so computed include: uniaxial orientational order S_A, (referred to the axial order in the system), the radial order S_R, (measuring the degree of alignment of liquid crystal molecules along the radial direction in the droplet, computed from $\langle P_2(\cos(\theta_i))\rangle$ where θ_i is the angle made by each of the liquid crystal molecules in the droplet with respect to the local radial direction and the angular brackets represent the ensemble average over the sample as well over the Monte Carlo runs), RMS fluctuations in these orders within each concentric layer, and the rigid lattice limit NMR spectrum of a deuterium (located on the core of the molecule) expected of the system assuming that the Zeeman field is always applied parallel to the instantaneous director. We take known typical values for deuterium quadrupole coupling constants (175 kHz) and the C-D bond angle with respect to the long axis of the molecule 60^o.

Canonical ensembles at the fixed reduced temperature of 0.01 (corresponding to K_1, K_2, and K_3 values of $7.0 \times 10^{-12}N$, 4.3×10^{-12}N, 17.0×10^{-12}N respectively and Λ = 710 $\mathring{A}$) were constructed for a droplet with a radius of 15 lattice units using the Markov chain Monte Carlo simulation based Metropolis algorithm. The data for computation of the above physical property's variables were collected over 5 million Monte Carlo steps after ignoring the first 1 million steps for equilibration. The results are discussed below.

6.3 Results and discussion

With the scale factor fixed at unity (i.e. using the typical values of the elastic coefficients of PAA as such), we see an anchoring mediated structural transition of the director configuration as depicted in figure 6.2. Both S_A and S_R show a sudden jump at $\varepsilon_S \sim 0.54$. When ε_S is close to zero, the surface does not have a significant influence on the director structure and the droplet has predominantly uniaxial director configuration represented by

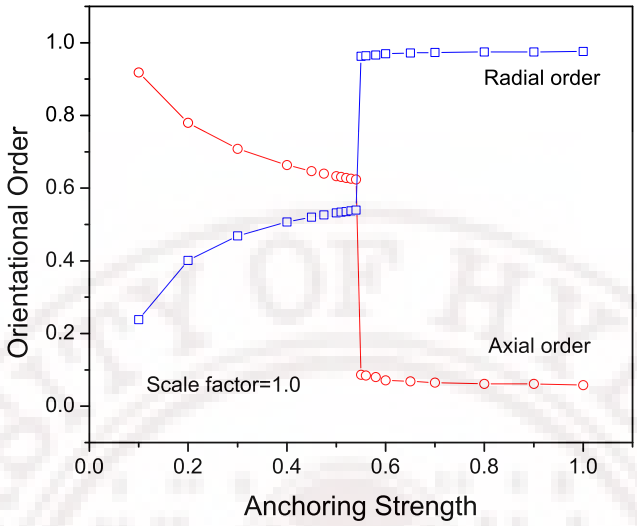

Figure 6.2: Variation of radial and axial order with anchoring strength for scale factor 1.00

a high value of S_A, and the corresponding S_R is low. As the value of ε_S is increased the uniaxial order decreases and at the threshold value of about 0.54 the axial order practically vanishes, while the radial order assumes a value very near unity. This would physically correspond to an anchoring mediated sudden change in the director structure finally culminating in an essentially radially ordered director configuration. These results are consistent with those of the earlier work carried out with LL model with $\varepsilon_S = 1$. It is interesting to see the corresponding changes in the layer-wise order parameters as a function of ε_S. These are depicted in figures 6.3 and 6.4. Both the figures, which are complementary, indicate that below the threshold ε_S the development of radial order, at the expense of the axial counterpart, is gradual as one moves out from the center of the droplet, and the droplet thus is getting gradually transforming from a pure uniaxial symmetry to a more spherical symmetry. Just at the threshold value, a sudden transition of the director structure takes place, making it essentially spherically symmetric, but for a small inner core (of a radius of about 3-4 lattice units) which still manages to have uniaxial order. This, is due to the significant elastic energy involved in forcing the radial orientations of the director to the very center of the droplet [23] [45]. Thus the minimum free energy is obtained by allowing a small core

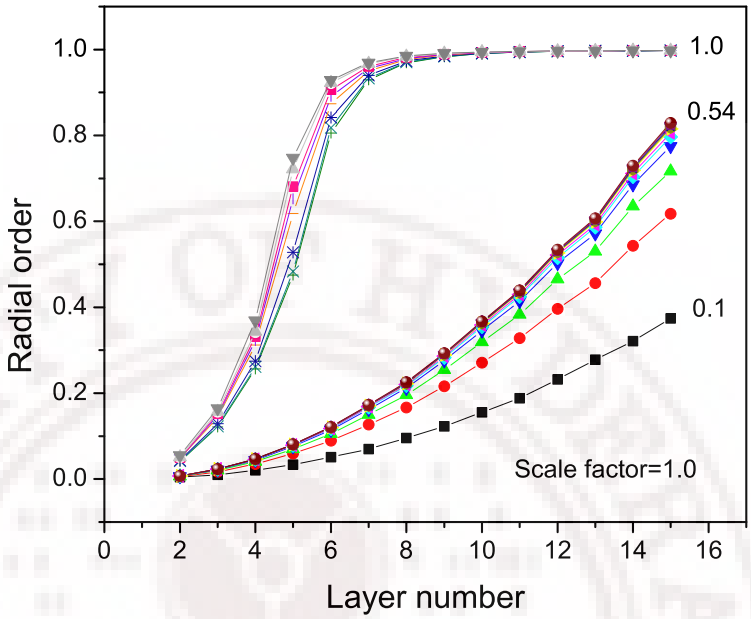

Figure 6.3: Variation of radial order with layers for the scale factor 1.00 for different anchoring strengths (the different plots correspond to different anchoring strengths ε_S, as indexed)

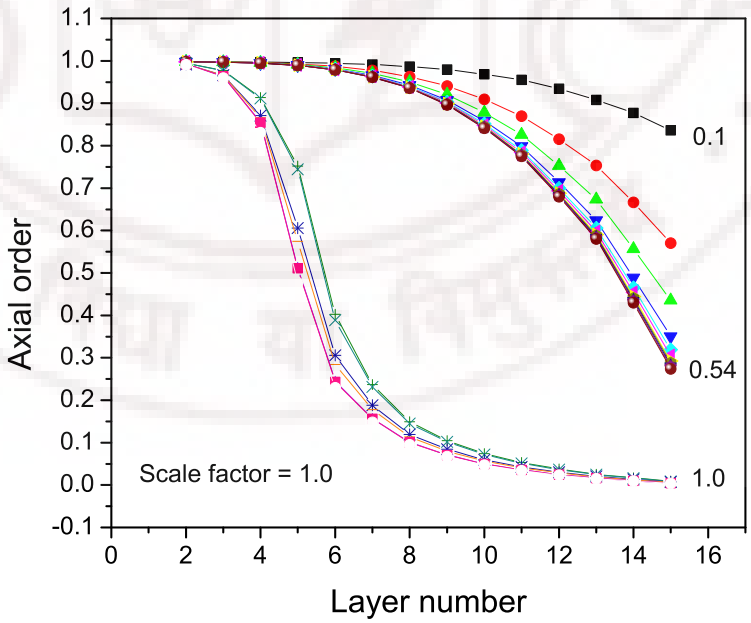

Figure 6.4: Variation of axial order with layers for the scale factor 1.00 for different anchoring strength (the different plots correspond to different anchoring strengths ε_S, as indexed)

of uniaxial region with some energy cost at the interface between two differently ordered regions of the medium.

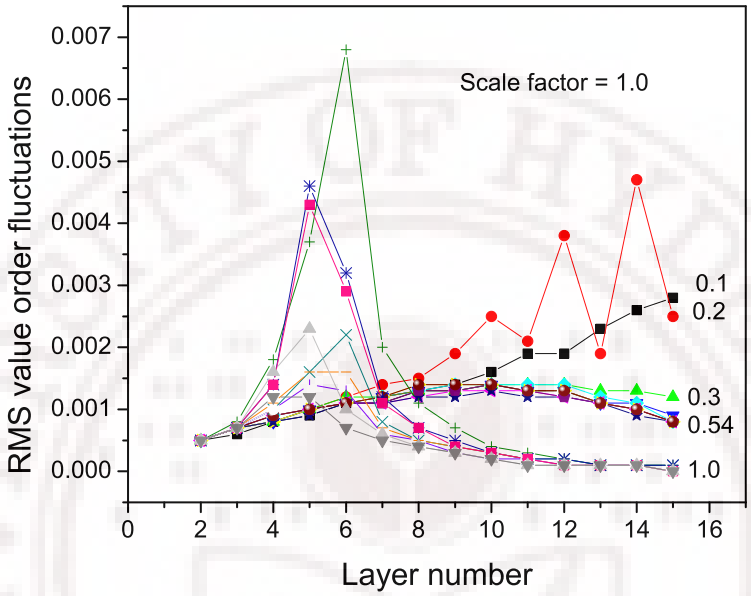

Figure 6.5: Variation of RMS value of order fluctuations with layer number for different anchoring strengths (the different plots correspond to different anchoring strengths ε_S, as indexed)

Figure 6.5 shows the RMS value of layer-wise (uniaxial) order fluctuations as ε_S is varied from 0.1 to 1.0. These fluctuations seem to provide an insight into the progression of the radial order towards the center, and are significant near the interfacial region at the delimiting surface due to frustration effects. When ε_S is low (0.1) the effect of radial anchoring seems to make the axial order fluctuate progressively more, as the confining surface is reached from the center. At $\varepsilon_S = 0.2$, there are very significant fluctuations which persist typically in the outer five layers, implying that at this anchoring value, the energy cost of percolating the radial order is competing with the interfacial energy (at the surface) involved to retain a large enough uniaxial region. It may be noted that this energy cost is relatively small at this large radius of the uniaxial droplet. However further increase of ε_S to 0.3, and up to a threshold value of about 0.54, indicates rather curiously that the fluctuations are uniform over the layers, but for a small (approximately two-fold) increase

in the middle layers of the droplet. This suggests that the uniaxial order fluctuations are smaller at the core (away from the competing boundary conditions) and at the surface (due to the pinning effect from the surface); and are somewhat more pronounced in the mid-layers, as can be expected under the circumstances. At the onset of the anchoring induced transition, beyond the threshold value of ε_S, however, the scenario changes qualitatively. The order fluctuations suddenly shift towards an inner layer (around 4-5 units) and show systematic peaks (unlike the fluctuations near the outer layers at $\varepsilon_S = 0.2$) at the interfacial surfaces, their position shifting progressively to inner layers as the anchoring strength is increased to unity beyond the threshold value. These fluctuations unambiguously show the onset of radial order, and its progression with anchoring strength; and provide the signature of the anchoring-induced structural transition in the medium. In order to correlate the above changes with experimentally observable quantities, ^2H NMR spectra expected from the different director configurations were generated for different ε_S values. Figure 6.6 shows two limiting spectra for ε_S = 0.1 and 1.0.

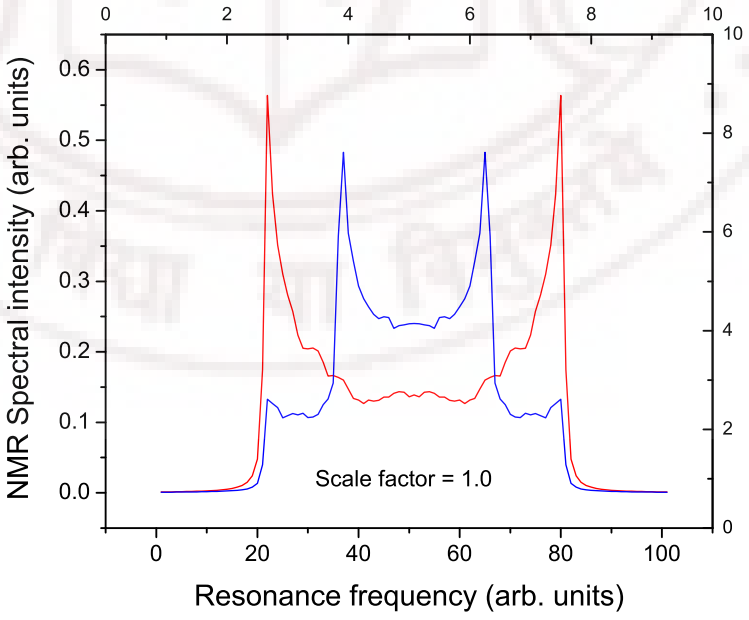

Figure 6.6: Simulated NMR spectrum for different resonant frequencies for the scale factor 1.00 (inner plot representing axial order).

The simulations were extended to find the effect of varying the energy cost of the relevant elastic distortion (*i.e.* splay constant K_1 relative to its actual value, while retaining the other two elastic constants the same) through the scale factor α, as mentioned before. Figure 6.7 shows the variation of the two orders with ε_S as α is varied from 0.1 to 3.0 in some convenient steps. It may be noted that after the onset of the anchoring-induced transition,

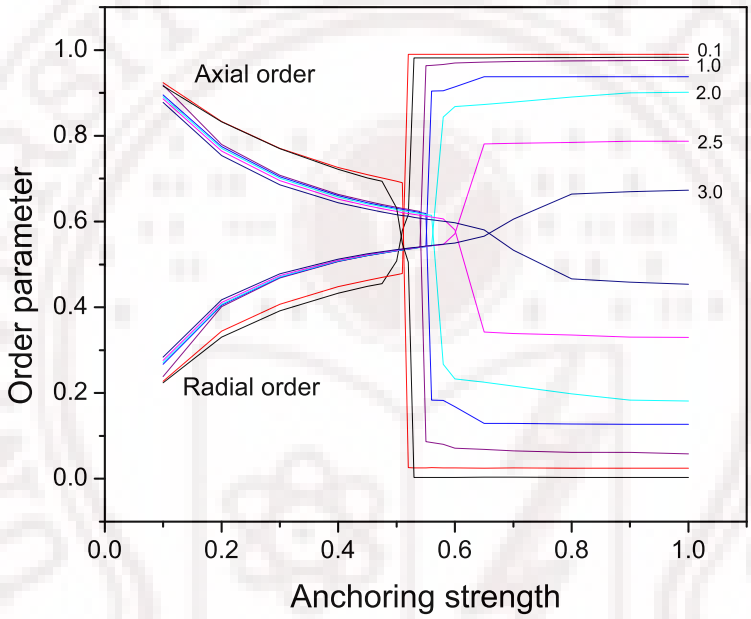

Figure 6.7: Variation of the order parameters with anchoring strength for different scale factors as indexed.

the region of interface between the uniaxial core and the outer radial region depends on the balancing of elastic energy costs involved, and in this case is determined by the splay elastic coefficient; other competing conditions kept constant. Thus, figure 6.7 shows that the effect of varying the relative value of the splay elastic constant is two fold: the threshold value for the anchoring transition increases with increase of α, and the extent of change in one type of order to the other type after the anchoring transition decreases with α. This is consistent with the picture that as K_1 is systematically increased, it requires more anchoring influence from the boundary to induce this transition, and a higher K_1 value also demands a larger uniaxial core for energy balance at the interface thus reducing the disparity between the

magnitudes of the two different types of orientational order. For comparison with the case of $\alpha = 1$ (figures 6.2 and 6.3), figures 6.8 and 6.9 show layer-wise variation of the two orders with ε_S at $\alpha = 0.1$. It is seen that the threshold value for the anchoring transition is now around 0.52 and the radius of the inner uniaxial core has diminished.

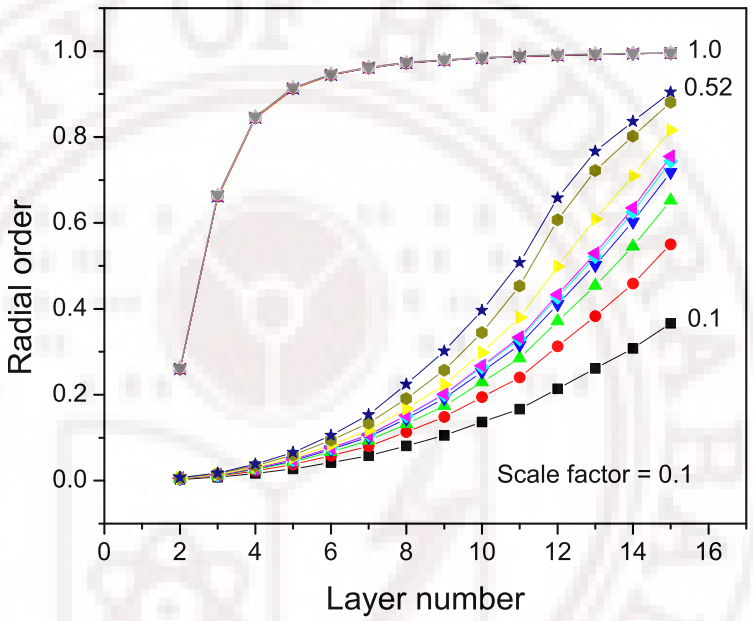

Figure 6.8: Radial order for every layer for the scale factor 0.1 for different anchoring strengths (the different plots correspond to different anchoring strengths ε_S, as indexed).

To examine the growth of the core region with uniaxial order as a function of changes in the splay constant, we show layer-wise variation of S_A as α is varied (figure 6.10). From this one can infer the typical size of the core sustaining uniaxial order and its dependence on splay elasticity. These results are plotted in figure 6.11 showing a linear variation of the radius of the spherical inner uniaxial core with scale factor α. From these results, one can also plot the variation of the threshold values of ε_S needed to induce the anchoring transition, as a function of different scale factor values (α), and thus is shown in figure 6.12. It is also illustrative to compute the ^2H NMR spectra for the different values of α, at the fixed $\varepsilon_S = 1$, to see how the corresponding layer-wise variation of the director field (figure 6.10) would reflect in an experimental situation, and this is shown in figure 6.13. To

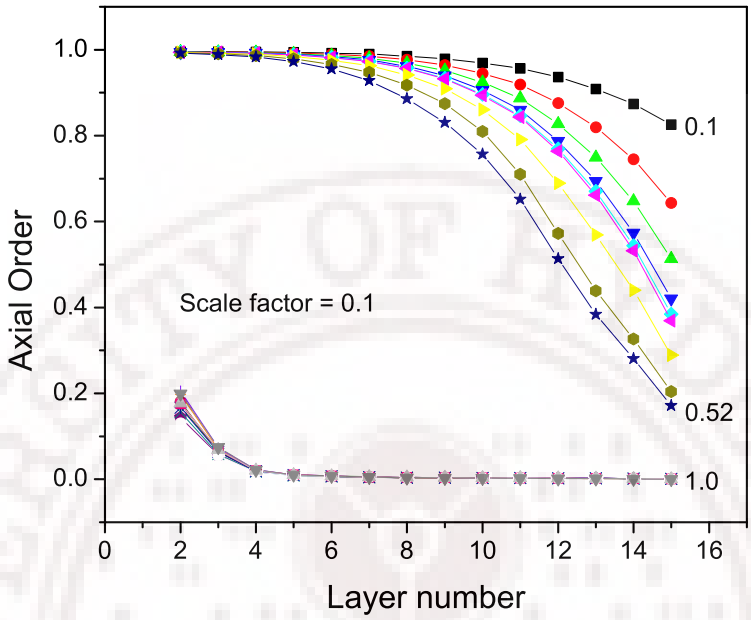

Figure 6.9: Axial order for different anchoring strength for every layer at scale factor 0.1 (the different plots correspond to different anchoring strengths ε_S, as indexed)

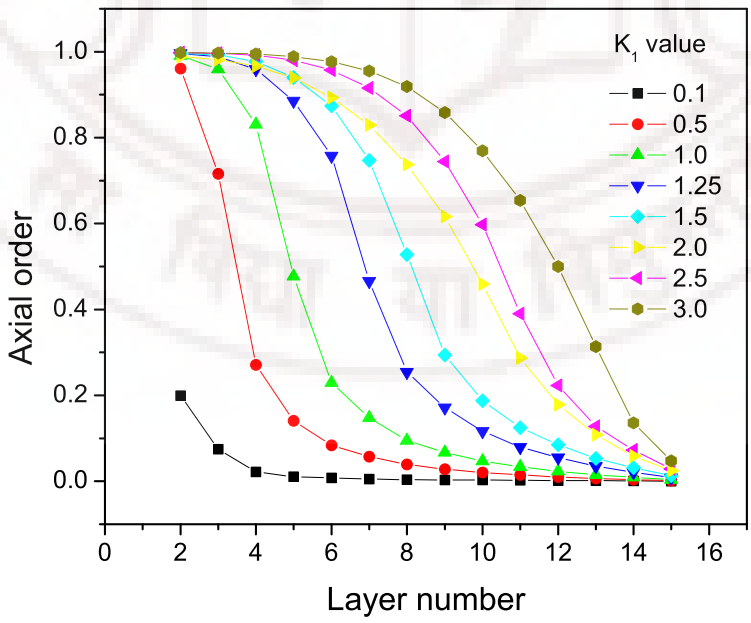

Figure 6.10: Variation of axial order for different K1 with the layer number.

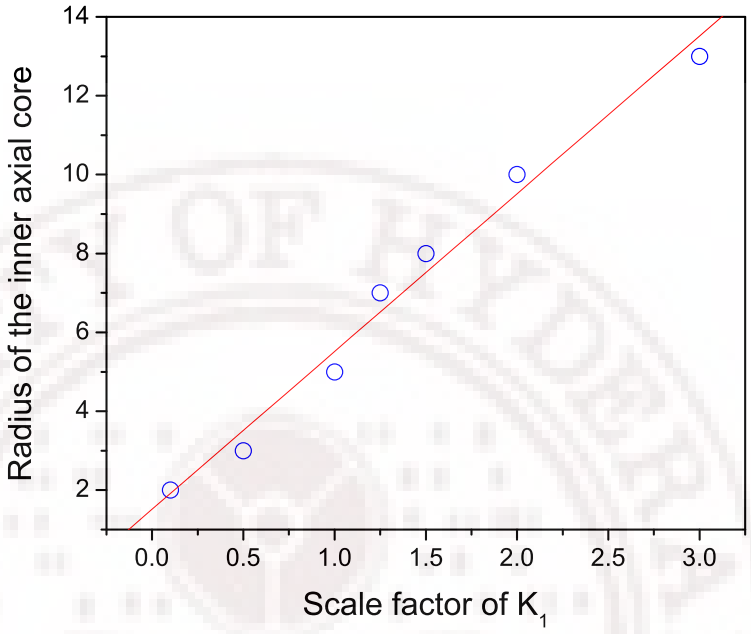

Figure 6.11: Radius of the inner axial order core with the scale factor

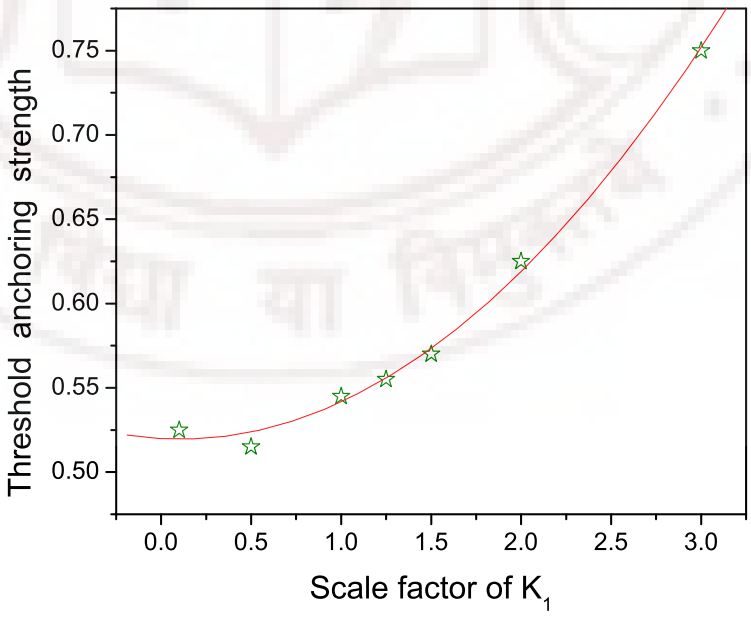

Figure 6.12: Variation of threshold anchoring strength with scale factor

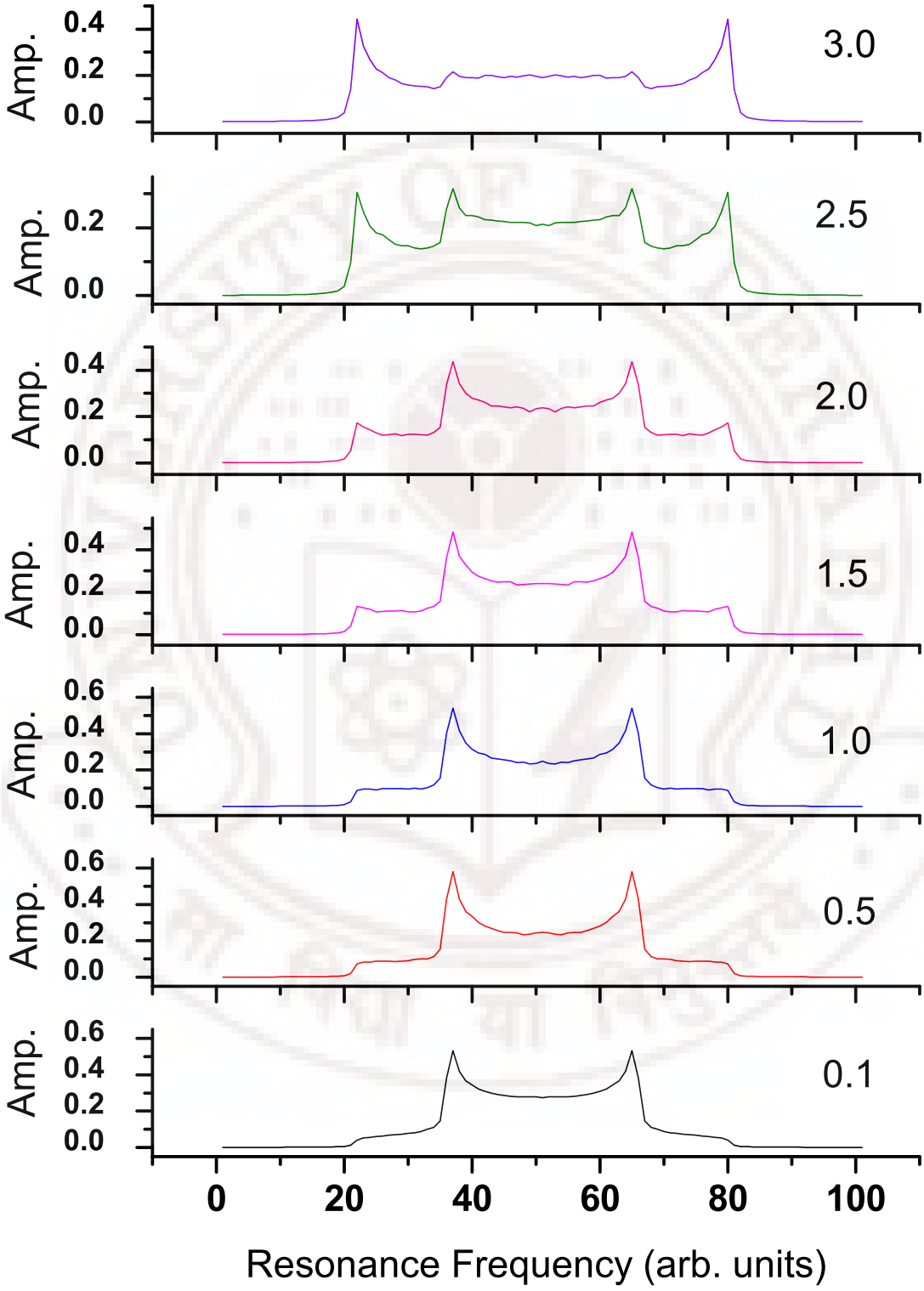

Figure 6.13: Simulated NMR spectra for various values of scale factors

look for possible hysteresis of this anchoring transition, given the abrupt changes induced by the anchoring strength, the simulations were repeated at $\alpha = 1$, by decreasing ε_S to zero starting from unity. The results are shown in figure 6.14 and it is observed that there is a strong hysteresis associated with this anchoring transition. The transition to the original uniaxial state (at the lower anchoring values) could not be located precisely, and one can only infer that it should be somewhere between 0.1 and 0.0.

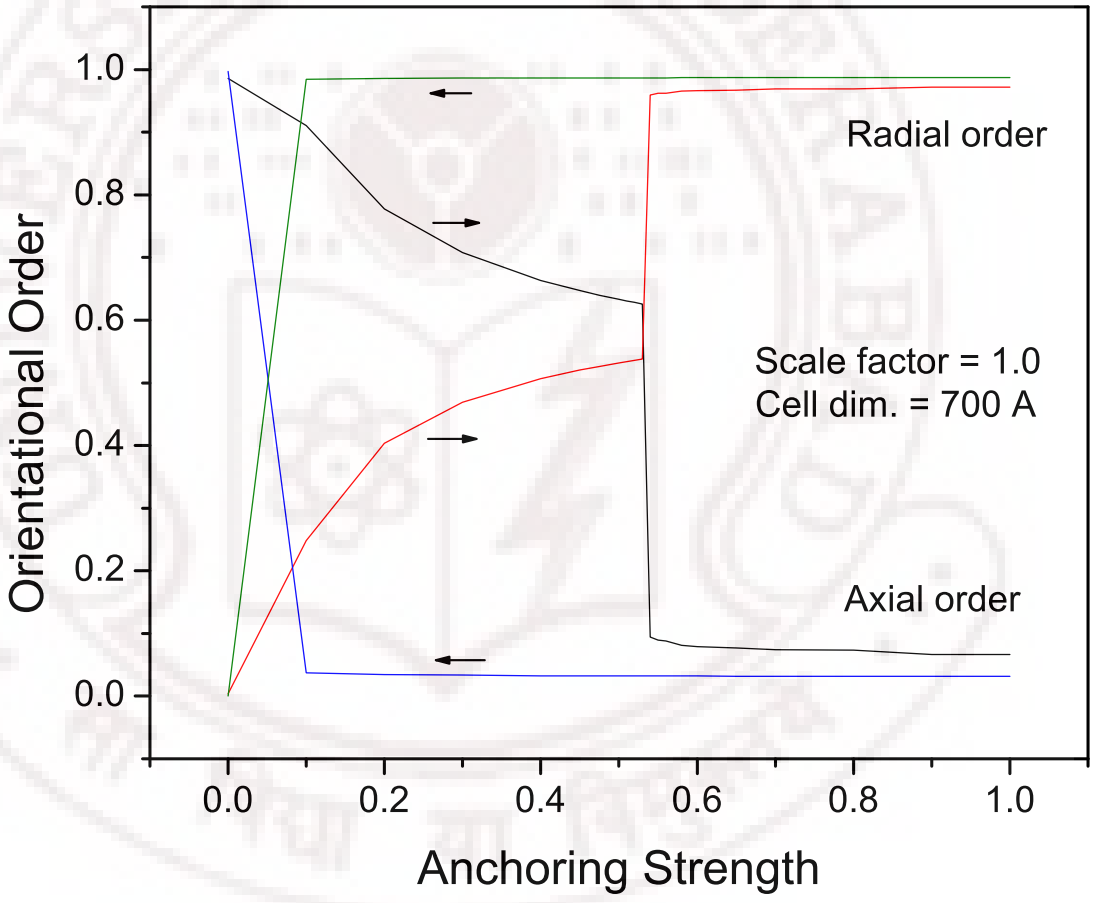

Figure 6.14: The hysteresis curve for cell dimension (Λ) 700 A

Finally, the applicability of this model depends on the the dimension of the volume element Λ chosen to represent the average director field, and it was held fixed at $700A^o$. To test limitations of this dimension on the results, simulations were also carried out, (setting $\alpha = 1$), at two other values of $\Lambda(70\mathring{A}$ and $7\mathring{A})$, and figure 6.15 summarizes the findings.

At $70\mathring{A}$ (corresponding to the reduced temperature of 0.1, it could be expected from the earlier work on planar hybrid films [44] that the volume element is too small to provide statically reliable representative director orientations (in statistical terms, the ensemble is collected at an unacceptably higher temperature), and any departures, if observed, were explained as due to the effect of large director fluctuations. The present results thus show that at lower values of Λ the effect of director fluctuations is considerable, and the transition displays a shift in the threshold anchoring strength and also apparent weakening of the transition (figure 6.15). The data at an even lower value shown in figure 6.15 proves this point convincingly.

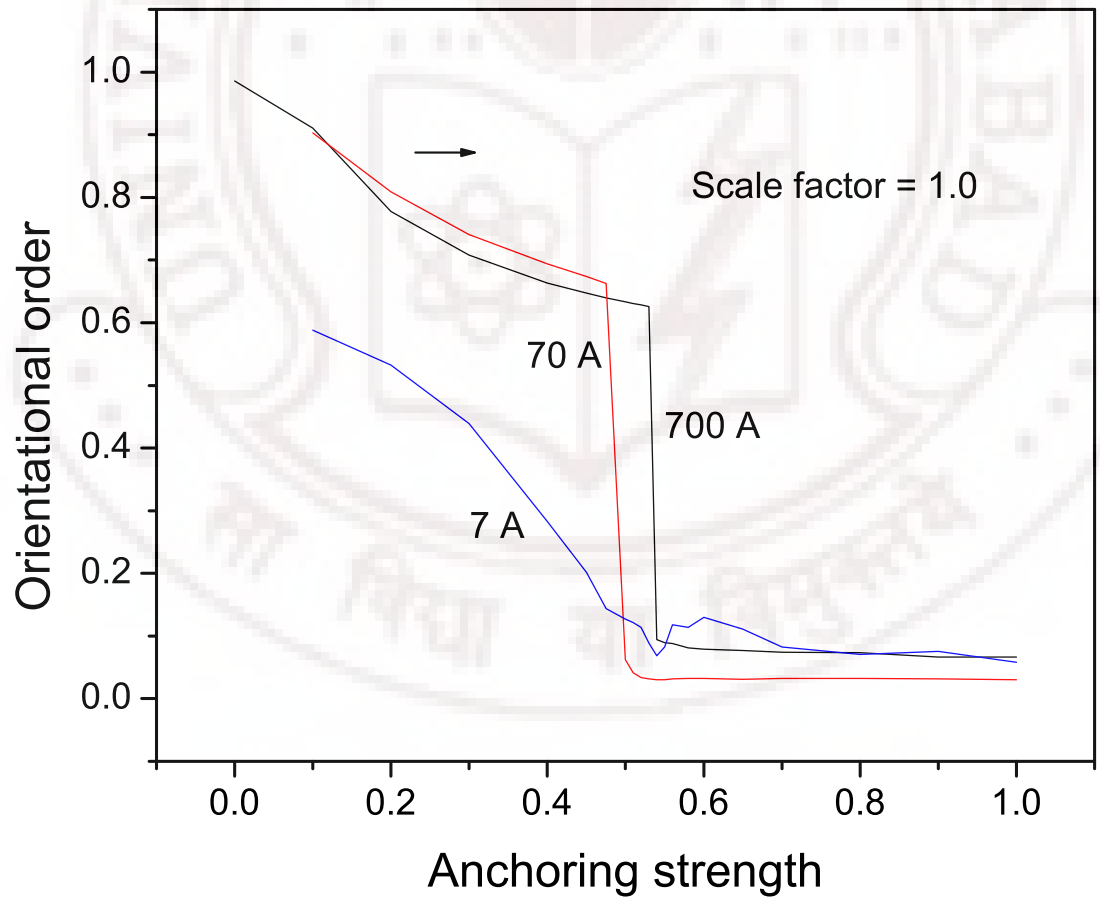

Figure 6.15: Variation of Orientational order with anchoring strength for different cell dimensions

6.4 Conclusions

Liquid crystal micro-droplet is revisited with a different Hamiltonian model which permits explicit incorporation of the elastic properties of the medium, under certain conditions. We report here a structural transition in the director field, induced by tuning the anchoring strength at the spherical boundary. The layer-wise profiles of the two orders which distinguish the two phases, as well as their layer-wise fluctuations, provide an insight into the progression of this transition. The flexibility of this model is used to simulate the effect of assigning different splay properties of the medium (via the scale parameter), and the anchoring transition is studied as a function of the scale parameter, keeping other conditions the same. This affects both the anchoring threshold for the transition, as well as the extent to which the radial order could penetrate into the droplet. These effects can be conveniently gleaned by looking at ^2H NMR spectra (under rigid lattice conditions) which represent the variations of the director fields more transparently. The anchoring transition seems to be of strong first order leading to complete wetting, and is reflected by the large hysteresis associated with this transition. This model is of course limited by the choice of the length scale connecting the volume element over which the local director is defined, and is effectively reflected in the Monte Carlo simulation via the reduced temperature that is assigned during the simulation. These limits are also examined to see the effect of director fluctuations on the anchoring transition reported.

Bibliography

[1] C.P.Grawford and S.Zummer. *Liquid crystal in complex geometries formed by polymer and porous network.* Taylor and Francis, London, 1996.

[2] J. W. Doane, A. Golemme, J. L. West, and J. B. Whitehead Jr.and B.G.Wu. Polymer dispersed liquid crystals for display application. *Mol. Cryst. Liq. Cryst*, 165:511–532, 1988.

[3] A.Golemme, S.Zumer, J.W.Doane, and M.E.Neubert. Deuterium nmr of polymer dispersed liquid crystal. *Phys. Rev. A*, 37(2):559, 1988.

[4] M. Ambrozic, P. Formoso, A. Golemme, and S. Zumer. Anchoring and droplet deformation in polymer dispersed liquid crystals:nmr study in an electric field. *Phys. Rev. E*, 56(2):1825, 1997.

[5] Ichiro Amimori, James N. Eakin, Gregor Skaej Jun Qi, Slobodan umer, and Gregory P. Crawford. Surface-induced orientational order in stretched nanoscale-sized polymer dispersed liquid-crystal droplets. *Phys. Rev. E*, 71:031702, 2005.

[6] J.W.Doane, N.A.Vaz, B.G.Wu, and S.Zumer. Field controlled light scattering from nematic droplets. *Appl. Phys. Lett.*, 48(4):269, 1986.

[7] G. Chidichimo, G. Arabia, A. Golemme, and J. W. Doane. Electrooptic properties of polymer dispersed liquid crystals. *Liquid Crystals*, 5(5):1443–1452, 1989.

[8] Nuno A. Vaz, George W. Smith, and G. Paul Montgomery Jr. A light control film composed of liquid crystal droplets dispersed in a uv-curable polymer. *Molecular Crystals and Liquid Crystals*, 146:1–15, 1987.

[9] Ichiro Amimori, Nikolai V. Priezjev, Robert A. Pelcovits, and Gregory P. Crawford. Optomechanical properties of stretched polymer dispersed liquid crystal films for scattering polarizer applications. *J. Of Appl. Phys.*, 93(6):3248, 2003.

[10] Marija Vilfan, Bostjan Zalar, Adam K. Fontecchio, Mojca Vilfan, Michael J. Escuti, Gregory P. Crawford, and Slobodan Zumer. Deuteron nmr study of molecular ordering in a holographic-polymer-dispersed liquid crystal. *Phys. Rev. E*, 66:021710, 2002.

[11] Chris C. Bowley, Pavel A. Kossyrev, Gregory P. Crawford, and Sadeg Faris. Variable-wavelength switchable bragg gratings formed in polymer-dispersed liquid crystals. *Appl. Phys. Lett.*, 79(1):9, 2001.

[12] Thein Kyu, Domasius Nwabunma, and Hao-Wen Chiu. Theoretical simulation of holographic polymer-dispersed liquid-crystal films via pattern photopolymerization-induced phase separation. *Phys. Rev. E*, 63:061802, 2001.

[13] J. Bajc and S. Zumer. Structural transition in chiral nematic liquid crystal droplets in an electric field. *Phys. Rev. E*, 55(3):2925, 1997.

[14] J. Bezic and S. Zumer. Structures of cholesteric liquid crystal droplets with parallel surface anchoring. *Liquid crystal*, 11(4):593419, 1992.

[15] S.Kralj and S.Zumer. Freedericksz transition in supra-μm nematic droplets. *Phys. rev. A*, 45(4):2461, 1992.

[16] S.Zumer. Light scattering from nematic droplets: Anomalous-diffraction approach. *Phys. Rev. A*, 37(10):4006, 1988.

[17] I.Vilfan, M.Vilfan, and S.Zumer. Orientational order in bipolar nematic microdroplets close to phase transition. *Phys. Rev. A*, 40(8):4724, 1989.

[18] S.Kralj, S.Zumer, and D.W.Allender. Nematic-isotropic phase transition in a liquid crystal droplet. *Phys. Rev. A*, 43(6):2943, 1991.

[19] S.Zumer and J.W.Doane. Light scattering from small nematic droplets. *Phys. Rev. A*, 34(4):3373, 1986.

[20] P. Pasini, C. Chiccoli, and C. Zannoni. *Advances in the Computer Simulations of Liquid Crystals*. Kluwer, Dordrecht, 2000.

[21] C. Chiccoli, P. Pasini, F. Semeria, T.J. Sluckin, and C. Zannoni. *J. Phys. II France*, 5:427, 1995.

[22] E. Berggren, C. Zannoni, C. Chiccoli, P. Pasini, and F. Semeria. Monte carlo study of the molecular organization in model nematic droplets-field effects. *Chem. Phys. Lett.*, 197:224–230, 1992.

[23] C. Chiccoli, P. Pasini, F. Semeria, and C. Zannoni. A computer simulation of nematic droplets with radial boundary conditions. *Phys. Lett. A*, 150:311–314, 1990.

[24] E. Berggren, C. Zannoni, C. Chiccoli, P. Pasini, and F. Semeria. Computer simulations of nematic droplets with bipolar boundary conditions. *Phys. Rev. E*, 50:2929–2939, 1994.

[25] C. Chiccoli, P. Pasini, F. Semeria, and C. Zannoni. Computer simulations of nematic droplets with toroidal boundary conditions. *Mol. Cryst. Liq. Cryst.*, 221:19–28, 1992.

[26] C. Chiccoli, P. Pasini, G. Skacej, S. Zumer, and C. Zannoni. *Lattice spin models of polymer-dispersed liquid crystals in Computer Simulations of liquid crystals and polymers*. Kluwer, Dordrecht, 2005.

[27] F. Biscarini, C. Chiccoli, P. Pasini, F. Semeria, and C. Zannoni. Phase diagram and orientational order in a biaxial lattice model. a monte carlo study. *Phys. Rev. Lett.*, 75:1803, 1995.

[28] C. Chiccoli, P. Pasini, I. Feruli, and C. Zannoni. Biaxial nematic droplets and their optical textures. a lattice model computer simulation study. *Mol. Cryst. Liq. Cryst.*, 441:319–328, 2005.

[29] Renate Onris-Crawford, Evan P. Boyko, Brian G. Wagner, John H. Erdmann, Slobodan Zumer, and J. William Doane. Microscope textures of nematic droplets in polymer dispersed liquid crystals. *J. Appl. Phys.*, 69(9):6380, 1991.

[30] P.A. Lebwohl and G. Lasher. Nematic-liquid-crystal ordera monte carlo calculation. *Phys. Rev. A*, 6:426, 1972.

[31] C. Chiccoli, P. Pasini, F. Semeria, and C. Zannoni. Monte carlo simulations of model nematic droplets. *Mol. Cryst. Liq. Cryst.*, 212:197–204, 1992.

[32] E. Berggren, C. Zannoni, C. Chiccoli, P. Pasini, and F. Semeria. Monte carlo study of the effect of an applied field on the molecular organization of polymer-dispersed liquid-crystal droplets. *Phys. Rev. E*, 49:614–622, 1994.

[33] A.P.J. Emerson and C. Zannoni. A monte carlo study of gay-berne liquid crystal droplets. *J. Chem. Soc. Faraday Trans.*, 91:3441–3447, 1995.

[34] C. Chiccoli, P. Pasini, G. Skacej, C. Zannoni, and S. Zumer. Nmr spectra from monte carlo simulations of polymer dispersed liquid crystals. *Phys. Rev. E*, 60:4219–4225, 1999.

[35] C. Chiccoli, P. Pasini, G. Skacej, C. Zannoni, and S. Zumer. Dynamical and field effects in polymer dispersed liquid crystals: Monte carlo simulations of nmr spectra of pdlc. *Phys. Rev. E*, 62:3766–3774, 2000.

[36] C. Chiccoli, Y. Lansac, P. Pasini, J. Stelzer, and C. Zannoni. Effect of surface orientation on director configurations in a nematic droplet. a monte carlo simulation. *Mol. Cryst. Liq. Cryst.*, 372:157–165, 2001.

[37] C. Chiccoli, P. Pasini, G. Skacej, C. Zannoni, and S. Zumer. Inhomogeneous translational diffusion in polymer dispersed liquid crystals: Monte carlo simulations of nmr spectra. *Mol. Cryst. Liq. Cryst.*, 367:2987–2997, 2001.

[38] L.V. Mirantsen and S. Romano. Molecular dynamics simulation of polymer dispersed liquid crystal droplets under competing boundary conditions. *Liquid Crystals*, 33(2):187194, 2006.

[39] C. Chiccoli, P. Pasini, F. Semeria, and C. Zannoni. A detailed monte carlo investigation of the tricritical region of a biaxial liquid crystal system. *Int. J. Mod. Phys. C*, 10:469–476, 1999.

[40] S. Romano. *Int. J. mod. Phys. B*, 12:2305, 1998.

[41] K. P. N. Murthy. *Monte Carlo methods in Satistical Physics*. Universities Press, 2003.

[42] T. Gruhn and S. Hess. *Z. Naturforsch.*, A51:1, 1996.

[43] G.R. Luckhurst and S. Romano. Computer simulation study of a nematogenic lattice model based on an elastic energy mapping of the pair potential. *Liq. Cryst.*, 26:871, 1999.

[44] P.J. Le Masurier, G.R. Luckhurst, , and G. Saielli. Monte carlo lattice simulations of the elastic behaviour of nematic liquid crystals. *Liq. Cryst.*, 28:769, 2001.

[45] N. Schopohl and T.J. Sluckin. *J. Physique*, 49:1097, 1988.